A Journal of the Gesellschaft Deutscher Chemiker

Angewandte International Edition

GDCh

Chemie

www.angewandte.org

Accepted Article

Title: Highly Efficient Electroreduction of CO2 to Methanol on Palladium-Copper Bimetallic Aerogels

Authors: Lu Lu, Xiaofu Sun, Jun Ma, Dexin Yang, Haihong Wu, Bingxing Zhang, Jianling Zhang, and Buxing Han

To be cited as: *Angew. Chem. Int. Ed.* 10.1002/anie.201808964
Angew. Chem. 10.1002/ange.201808964

Link to VoR: http://dx.doi.org/10.1002/anie.201808964
http://dx.doi.org/10.1002/ange.201808964

WILEY-VCH

10.1002/anie.201808964

WILEY-VCH

Highly Efficient Electroreduction of CO_2 to Methanol on Palladium-Copper Bimetallic Aerogels

Lu Lu,[a,b] Xiaofu Sun,[a,b]* Jun Ma,[a] Dexin Yang,[a,b] Haihong Wu,[c] Bingxing Zhang,[a,b] Jianling Zhang,[a,b] Buxing Han[a,b]*

Abstract: Electrochemical reduction of CO_2 to CH_3OH is a very interesting topic. Aerogels are fine inorganic superstructure with high porosity and are known to be exceptional materials. Here we developed a Pd-Cu bimetallic aerogel electrocatalyst for conversion of CO_2 into CH_3OH. The current density and Faradaic efficiency of CH_3OH can be as high as 31.8 mA cm^{-2} and 80.0% over $Pd_{83}Cu_{17}$ aerogel at a very low overpotential (0.24 V). The superior performance of the electrocatalyst results from efficient adsorption and stabilization CO_2 radical anion, high Pd^0/Pd^{II} and Cu^I+Cu^0/Cu^{II} ratios and sufficient Pd/Cu grain boundaries of aerogel nanochains.

CO_2 is the main greenhouse gas, and also a cheap, non-toxic, and abundant C1 feed stock.[1] The interest in electrochemical CO_2 reduction reaction (CO_2RR) has sparked a sustained research effort. In recent years, many electrocatalysts has been studies, including metals, metal oxides, transition-metal chalcogenides and carbon-based materials.[2-7] In particular, numerous efforts have been dedicated to developing and improving the performance of metal catalysts for CO_2RR,[8,9] among which controlling the size, shape and morphology of nanostructured metals is an effective strategy.[10] However, substantial advances for searching new electrodes in CO_2RR are still needed to meet the criteria for practical applications.

Generally, Cu is the unique metal electrochemical catalyst that is capable of reducing CO_2 to a series of hydrocarbons, acids and alcohols with comparative Faradaic efficiency.[10] But there are still some drawbacks for Cu electrodes for CO_2RR, such as high overpotential, wide product distribution and a severe competing reaction of hydrogen evolution.[11] Many efforts have been devoted to improving the selectivity and current density for CO_2RR to a specific product over Cu-based catalysts, including designing Cu complexes, nanoscale Cu, oxide-derived Cu and alloying.[12-15] In comparison with Cu, Pd have low overpotential for CO_2 reduction, but CO or HCOOH are usually the major product,[16] and hardly reduced to alcohols with high Faradaic efficiency.

Different strategies have been developed to increase the activity of bimetallic catalysts, such as alloy, shape control, surface modification and oxidative treatment.[17-20] Recently, mesoporous Pd-Cu bimetallic electrodes were reported to be efficient for selective electrocatalytic CO_2RR to CO.[21] Cu-modified Pd catalyst was demonstrated to improve the Faradaic efficiency of HCOOH.[22] As a synergistic catalyst, polymer-supported Pd-Cu nanoalloy can enhance the ability for CO_2 reduction to CH_4.[23] Pd-Cu catalysts with ordered, disordered, and phase-separated atomic arrangements also have different selectivities to CO/hydrocarbons.[24] However, the use of Pd-Cu bimetallic electrode for CO_2RR to CH_3OH with a satisfactory selectivity has not been reported (Table S1).

Aerogels are fine inorganic superstructure with enormously high porosity and are known to be exceptional materials with a variety of applications, especially for catalysis. The physical and chemical properties of aerogel materials are often superior to the conventional nanoparticles since the specific properties of the nanomaterials are combined and magnified by self-assembly on the macroscale.[25,26] As a unique class of aerogels, Pd-based aerogels have attracted great interest. They can be used as unsupported electrocatalysts to offer enhanced overall catalyst activity and high stabilities.[25] Hence, appropriate Pd-based bimetallic aerogels may have potential application in CO_2RR.

Herein, we report the first work to use bimetallic aerogels as the catalysts for CO_2 electroreduction. We prepared a serious of Pd_xCu_y bimetallic aerogels with controlled composition *via* a template-free self-assembly process. By using $Pd_{83}Cu_{17}$ bimetallic aerogels on carbon paper (CP) as electrode and 1-butyl-3-methylimidazolium tetrafluoroborate ([Bmim]BF_4) aqueous solution as electrolyte, the Faradaic efficiency for CH_3OH production could reach 80.0 % with a current density of 31.8 mA cm^{-2}, which is higher than those reported in the literature.[27-30] The varying composition in Pd_xCu_y aerogels resulted in different Pd^0/Pd^{II} and Cu^I+Cu^0/Cu^{II} radios, which was found to be correlated with the CO_2 electrocatalytic activity and CH_3OH selectivity. Moreover, the special nanochain structure of aerogels also contributed to the enhancement of Pd/Cu grain boundaries and CH_3OH production.

Pd_xCu_y aerogels were obtained via in situ reduction of metal precursors and supercritical CO_2 ($scCO_2$) drying (Figure S1). We varied the mole ratios of Pd and Cu precursors to prepare a series of Pd_xCu_y (Table S2). Strong Pd and Cu peaks can be observed from X-ray photoelectron spectroscopy (XPS) spectra of the $Pd_{83}Cu_{17}$ aerogel in Figure S2. Scanning electron microscopy (SEM) and transmission electron microscopy (TEM) images (Figure 1A and 1B) show that $Pd_{83}Cu_{17}$ aerogel has a typical three-dimensional porous architecture with interconnected nanowires. High-resolution (HR) TEM images (Figure 1C) show that $Pd_{83}Cu_{17}$ aerogels are fairly uniform with an average nanowire diameter of about 6 nm. The lattice spacing presented in Figure 1D is about 0.22 nm corresponding to (111) interplane distance of face-centered cubic (fcc) Pd. Obvious metal segregation can be seen, and the amorphous parts belonged to amorphous Cu. The element mapping analysis and line-scan analysis were performed (Figure 1E-H), revealing presence of Pd and Cu in the aerogel. The typical

[a] L. Lu, Dr. X. Sun, Dr. J. Ma, D. Yang, B. Zhang, Prof. Dr. J. Zhang, Prof. Dr. B. Han.
Beijing National Laboratory for Molecular Sciences, Key Laboratory of Colloid and Interface and Thermodynamics, Research/Education Center for Excellence in Molecular Sciences, Institute of Chemistry, Chinese Academy of Sciences, Beijing 100190 (China)
E-mail: hanbx@iccas.ac.cn, sunxiaofu@iccas.ac.cn
[b] L. Lu, Dr. X. Sun, D. Yang, B. Zhang, Prof. Dr. J. Zhang, Prof. Dr. B. Han.
School of Chemistry and Chemical Engineering, University of Chinese Academy of Sciences, Beijing 100049 (China)
[c] Prof. Dr. H. Wu, Shanghai Key Laboratory of Green Chemistry and Chemical Processes, School of Chemistry and Molecular Engineering, East China Normal University, Shanghai 200062 (China)

Supporting information for this article is given via a link at the end of the document.

selected-area electron diffraction (SAED) patterns of $Pd_{83}Cu_{17}$ aerogel is shown in Figure 1I. Compared with pure Pd, no change of the corresponding radius of diffraction ring of $Pd_{83}Cu_{17}$ aerogel was observed, indicating that the aerogel was not alloy. According to X-ray diffraction (XRD) (Figure 1K), the peaks can be assigned to (111), (200), (220) and (311) planes of fcc Pd, which is consistent with SAED pattern. No distinct shift of peak position was observed on $Pd_{83}Cu_{17}$ aerogel relative to Pd metal (JCPDS# 65-6174), further suggesting that the bimetallic nanostructures were composed of crystallized Pd and amorphous Cu rather than PdCu alloy.

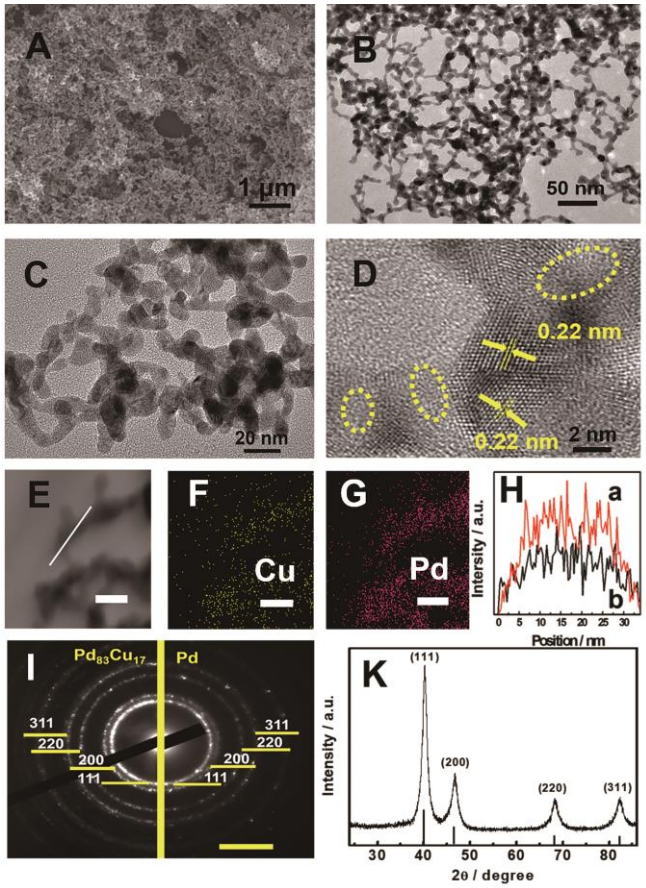

Figure 1. A) SEM, B, C) TEM, D) HR-TEM, E-G) EDX mapping images (scale bar: 20 nm). H) Distribution of the Pd (a) and Cu (b) in $Pd_{83}Cu_{17}$ by line-scan analysis. I) SAED pattern of the $Pd_{83}Cu_{17}$ and pure Pd (scale bar: 10 1/nm). K) XRD pattern of $Pd_{83}Cu_{17}$ aerogel.

The surface areas estimated from Brunauer-Emmett-Teller (BET) plots are 72.8, 65.7, 72.7, 76.8 and 76.9 m^2g^{-1} for $Pd_{83}Cu_{17}$, $Pd_{89}Cu_{11}$, $Pd_{87}Cu_{13}$, $Pd_{71}Cu_{29}$ and $Pd_{67}Cu_{33}$ aerogels, respectively (Figure S3). All the aerogels show a broad range of pores from micropores to mesopores. Besides, SEM, TEM images and XRD petterns of other Pd_xCu_y are shown in Figures S4-S5. All of them have similar three-dimensional porous architectures morphology with a bimetallic nanostructure rather than alloy.

The electrocatalytic performances of Pd_xCu_y aerogels were investigated in CO_2-saturated $[Bmim]BF_4$ aqueous solution with 25 mol% $[Bmim]BF_4$ and 75 mol% water by using a H-type cell.[6] The linear sweep voltammetry (LSV) curves for Pd_xCu_y aerogels are shown in Figure 2A. The applied potential was swept between -0.6 V and -2.5 V (vs. Ag/Ag^+) at a sweep rate of 20 mV s^{-1}. The overall current density also contains hydrogen evolution reaction current.

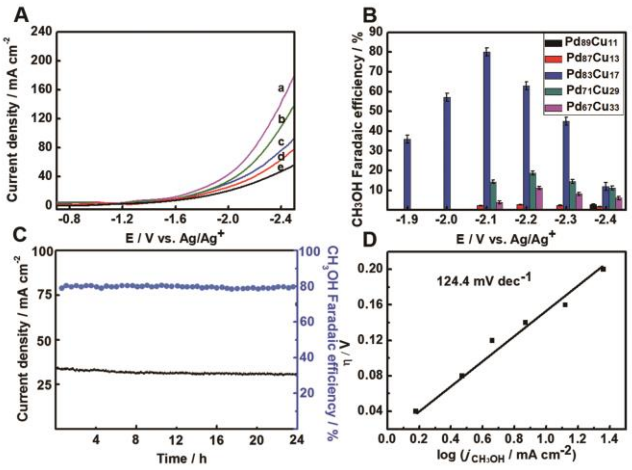

Figure 2. CO_2 electroreduction reactions in $[Bmim]BF_4$ aqueous solution with 25 mol% $[Bmim]BF_4$ and 75 mol% water. A) LSV curves for Pd_xCu_y aerogels: (a) $Pd_{67}Cu_{33}$, (b) $Pd_{71}Cu_{29}$, (c) $Pd_{83}Cu_{17}$, (d) $Pd_{87}Cu_{13}$, (e) $Pd_{89}Cu_{11}$. B) Faradaic efficiency for CH_3OH over Pd_xCu_y aerogels. C) Current density and Faradaic efficiency of long term electrolysis over $Pd_{83}Cu_{17}$ aerogel electrodes at -2.1 V vs. Ag/Ag^+. D) Tafel plots for CH_3OH production over $Pd_{83}Cu_{17}$ aerogel electrode.

Controlled potential electrolysis at each given potential was performed in the same system. The main gaseous product was H_2 and a trace amount of CO (<1 %) was determined by gas chromatography (GC). The electrolyte was analyzed by using ^1H NMR, showing that CH_3OH is the only liquid product. We also used $^{13}CO_2$ over the $Pd_{83}Cu_{17}$ aerogel in the same system. ^{13}C NMR spectra showed an obvious peak at 49.5 ppm, which is attributed to $^{13}CH_3OH$ (Figure S6A). ^1H NMR spectra indicated only $^{13}CH_3OH$ is produced (Figure S6B), and more discussion is given in the supporting information. These data confirm that CO_2 is the only carbon source for CH_3OH. Figure 2B shows the Faradaic efficiency of CH_3OH on Pd_xCu_y aerogels electrodes from -1.9 V to -2.4 V (vs. Ag/Ag^+). The proportion of Cu in Pd_xCu_y aerogels has a significant impact on the Faradaic efficiency of CH_3OH. We also studied the change of CH_3OH Faradaic efficiency at different potentials and electrolyte with different water mole fractions (Figure S7). The $Pd_{83}Cu_{17}$ shows the highest Faradaic efficiency for CH_3OH production (80.0 %) at -2.1 V (vs. Ag/Ag^+) in $[Bmim]BF_4$ aqueous solution with 25 mol% $[Bmim]BF_4$ and 75 mol% water after 5 h electrolysis. We also studied CO_2RR over $Pd_{87}Cu_{13}$ in 0.5 M $NaHCO_3$ and Na_2SO_4 aqueous solution, but only H_2 and a trace of HCOOH were detected.

The durability experiment over the $Pd_{83}Cu_{17}$ aerogel with long-time electrolysis was investigated at -2.1 V (vs. Ag/Ag^+) and the results are provided in Figure 2C. The current densities and Faradaic efficiency did not decrease during 24 h in the electrolysis. The difference of TEM images (Figure S8) of $Pd_{83}Cu_{17}$ aerogel before and after electrolysis is not notable. The XPS spectra of $Pd_{83}Cu_{17}$ after 24 h electrolysis determined in a UHV-XPS chamber (Figure S9-S10), further confirming the stability of aerogel. Besides, HR-TEM image of $Pd_{83}Cu_{17}$ after 24 h electrolysis (Figure S11) indicates that the nanostructure of fcc Pd and amorphous Cu did not change. The durability experiments of the other Pd_xCu_y aerogels (Figure S12) also suggest that they are stable during CO_2RR.

To gain kinetic insights for CO_2RR to CH_3OH on $Pd_{83}Cu_{17}$ aerogel, the current density for CH_3OH at various overpotentials were measured and Tafel plot was constructed in Figure 2D. A Tafel slope of was 124.4 mV dec^{-1} , which indicates the rate-determining step is the first electron transfer step ($CO_2 + e \rightarrow CO_2^{\bullet-}$), which is a commonly accepted mechanism over metal elecrtrodes.[31]

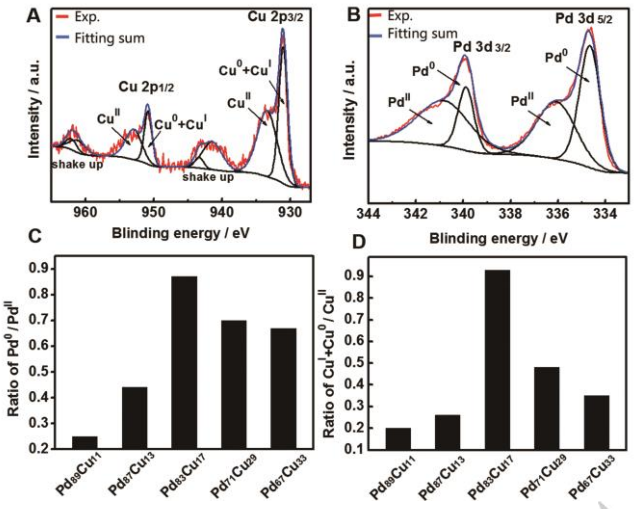

Figure 3. XPS spectra of A) Cu 2p level and B) Pd 3d level of catalysts. The relative intensity ratios of C) Pd^0/Pd^{II} and D) Cu^I+Cu^0/Cu^{II} in catalysts.

We characterized the electrocatalysts by XPS to get more information between surface electronic states and catalytic performance (Figure 3, Figure S13-S14). The Cu 2p spectra were fitted with two components, which are Cu^I+Cu^0 ($2p_{3/2}$, 931.1 eV; $2p_{1/2}$, 950.0 eV) and Cu^{II} ($2p_{3/2}$, 933.6 eV; $2p_{1/2}$, 953.2 eV). On the other hand, the intense Pd $3d_{5/2}$ peaks of $Pd_{83}Cu_{17}$ aerogel at 334.7 eV and 336.1 eV correspond to the metallic Pd^0 and Pd^{II}, and the Pd $3d_{3/2}$ peaks at 340.0 eV and 341.1 eV correspond to Pd^0 and Pd^{II}. The variation of the molar ratios of Pd and Cu in aerogels leads to different relative intensity ratio of Cu^I+Cu^0/Cu^{II} and Pd^0/Pd^{II} (Figure 3C-4D). $Pd_{83}Cu_{17}$ shows the highest Pd^0/Pd^{II} and Cu^I+Cu^0/Cu^{II} radio. This indicates that some O species exist on the aerogel surfuce, which may result mainly from the oxidation of the aerogels upon their exposure to air. The bimetallic nanostructures were composed of crystallized Pd (fcc) and amorphous Cu. Amorphous Cu had large amount of low-coordinated atoms and hence was abundant defects. Thus, more catalytic centers were created to enhance CO_2 catalytic performance.[32] In the meantime, the moderate O-modified Pd-Cu surface can be benefit to CO_2 chemical adsorption and subsequent hydrogenation in CO_2RR.[33-35] The CO_{ads} and CHO_{ads} can be also adsorbed efficiently on Cu^I+Cu^0 species,[36,37] resulting in the increasing of CH_3OH yields.

We also prepared the pure metal Pd and Cu by using the same method. However, Pd or Cu could not form hydrogel despite the sediments were obtained. As shown in Figure S15, the monometallic Cu had a flake-like morphology, and the monometallic Pd formed aggregated particles. We can conclude that both Cu and Pd are essential in the coalescence of the initial spherical particles into chainlike structures in the process of hydrogel formation. The Faradaic efficiencies and current densities for CO_2RR over monometallic Cu or Pd with different applied potentials after 5 h electrolysis are shown in Table S3-S4. CH_3OH was not detected at all applied potentials, indicating the excellent performance of aerogel is attributed to the synergistic effect between Pd and Cu.

We characterized the electrochemical activities of Pd_xCu_y aerogels according to the Randles-Sevcik equation. The reduction current density at -2.1 V (vs. Ag/Ag^+) plotted against the square root of scan rate are shown in Figure 4A. $Pd_{83}Cu_{17}$ aerogel electrode has largest slope, indicating the increased apparent concentration of reactant and highest electrochemical activity for CO_2RR. Additionally, the stabilization of reduced $CO_2^{\bullet-}$ intermediate plays an important role in CO_2RR to CH_3OH. Generally, the overpotential of SO_4^{2-} adsorption can be considered as a measure of binding strength of intermediates in the electrochemical reaction.[38] So we examined SO_4^{2-} adsorption as a surrogate on the Pd_xCu_y aerogels electrodes by measuring single oxidative LSV scans betweeen 0 and 1.7 V (vs. Hg/Hg_2SO_4) at 10 mV s^{-1} in N_2-saturated 0.1 M H_2SO_4 electrolyte, which can explore the binding affinity of the reduced intermediate $CO_2^{\bullet-}$ during CO_2RR. Based on the data in Figure 4B, the overpotential for $Pd_{83}Cu_{17}$ aerogel electrode is lowest, indicating largest binding energy and stronger binding of SO_4^{2-}. Hence the $Pd_{83}Cu_{17}$ aerogel electrode can stabilize $CO_2^{\bullet-}$ intermediates more efficiently.

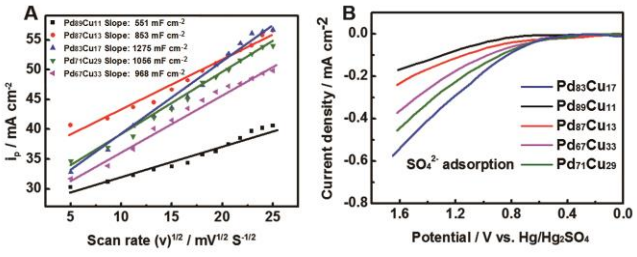

Figure 4. A) The reduction current density at -2.1 V (vs. Ag/Ag^+) plotted against the square root of scan rate for Pd_xCu_y aerogels. B) Single oxidative LSV curves for SO_4^{2-} adsorption in N_2-saturated 0.1 M H_2SO_4.

The high electrocatalytic activity of $Pd_{83}Cu_{17}$ aerogel is also ascribed to the highly porous non-supported network, which may

favor the exposure of electrochemical active sites and a good reactant flux. We also studied the influence of different drying method on the CO_2 electrocatalytic activity, including vacuum hot drying (HD) and freeze drying (FD) (Figure S16). Both the HD and FD sample show lower Faradaic efficiency for CH_3OH (9.6 % and 19.6 %) at -2.1 V (vs. Ag/Ag^+) (Figure S17).

In summary, the electrocatalytic reduction of CO_2 to CH_3OH has been studied over a series of Pd_xCu_y aerogels. The $Pd_{83}Cu_{17}$ aerogel electrode is very efficient and stable electrocatalyst. When 25 mol% $[Bmim]BF_4$ and 75 mol% water is used as electrolyte, the Faradaic efficiency of CH_3OH production can reach 80.0 % with a current density of 31.8 mA cm^{-2}. The excellent catalytic performance of the aerogel originates mainly from the synergistic effect between Pd and Cu with special valence states as well as the network structure of the aerogel. This work provides a promising method for electrolytic synthesis of CH_3OH from CO_2. We believe that other multimetallic aerogel catalysts can be designed for efficient CO_2RR to useful chemicals and fuels.

Acknowledgements

The authors thank National Key Research and Development Program of China (2017YFA0403102), the National Natural Science Foundation of China (21673248, 21733011, 21533011), and the Chinese Academy of Sciences (QYZDY-SSW-SLH013).

Keywords: carbon dioxide • electrocatalysis • aerogels • methanol • ionic liquids

[1] M. He, Y. Sun, B. Han, *Angew. Chem. Int. Ed.* **2013**, *52*, 9620-9633; *Angew. Chem.* **2013**, *125*, 9798-9812.

[2] Q. Zhu, J. Ma, X. Kang, X. Sun, H. Liu, J. Hu, Z. Liu, B. Han, *Angew. Chem. Int. Ed.* **2016**, *55*, 9012-9016; *Angew. Chem.* **2016**, *128*, 9158-9162.

[3] S. Gao, Y. Lin, X. Jiao, Y. Sun, Q. Luo, W. Zhang, D. Li, J. Yang, Y. Xie, *Nature* **2016**, *529*, 68-71.

[4] F. Li, L. Chen, G. P. Knowles, D. R. MacFarlane, J. Zhang, *Angew. Chem. Int. Ed.* **2017**, *56*, 505-509; *Angew. Chem.* **2017**, *129*, 520-524.

[5] G.-L. Chai, Z.-X. Guo, *Chem. Sci.* **2016**, *7*, 1268-1275.

[6] X. Sun, L. Lu, Q. Zhu, C. Wu, D. Yang, C. Chen, B. Han, *Angew. Chem. Int. Ed.* **2018**, *57*, 2427-2431; *Angew. Chem.* **2018**, *130*, 2451– 2455.

[7] W. Ma, H. Wang, W. Yu, X. Wang, Z. Xu, X. Zong, C. Li, *Angew. Chem. Int. Ed.* **2018**, *57*, 3473-3477; *Angew. Chem.* **2018**, *130*, 3531-3535.

[8] D. Gao, H. Zhou, J. Wang, S. Miao, F. Yang, G. Wang, J. Wang, X. Bao, *J. Am. Chem. Soc.* **2015**, *137*, 4288-4291.

[9] S. Liu, H. Tao, L. Zeng, Q. Liu, Z. Xu, Q. Liu, J.-L. Luo, *J. Am. Chem. Soc.* **2017**, *139*, 2160-2163.

[10] T. N. Huan, N. Ranjbar, G. Rousse, M. Sougrati, A. Zitolo, V. Mougel, F. Jaouen, M. Fontecave, *ACS Catal.* **2017**, *7*, 1520-1525.

[11] K. P. Kuhl, E. R. Cave, D. N. Abram and T. F. Jaramillo, *Energy Environ. Sci.* **2012**, *5,* 7050-7059.

[12] R. Angamuthu, P. Byers, M. Lutz, A. L. Spek, E. Bouwman, *Science* **2010**, *327*, 313-315.

[13] A. Loiudice, P. Lobaccaro, E. A. Kamali, T. Thao, B. H. Huang, J. W. Ager, R. Buonsanti, *Angew. Chem. Int. Ed.* **2016**, *55*, 5789-5792; *Angew. Chem.* **2016**, *128*, 5883-5886.

[14] S. Lee, D. Kim, J. Lee, *Angew. Chem. Int. Ed.* **2015**, *54*, 14701-14705; *Angew. Chem.* **2015**, *127*, 14914-14918.

[15] S. Sarfraz, A. T. Garcia-Esparza, A. Jedidi, L. Cavallo, K. Takanabe, *ACS Catal.* **2016**, *6*, 2842-2851.

[16] X. Min, M. W. Kanan, *J. Am. Chem. Soc.* **2015**, *137*, 4701-4708.

[17] A. Loiudice, P. Lobaccaro, E. A. Kamali, T. Thao, B. H. Huang, J. W. Ager, R. Buonsanti, *Angew. Chem. Int. Ed.* **2016**, *55*, 5789-5792; *Angew. Chem.* **2016**, *128*, 5883–5886.

[18] S. Zhang, P. Kang, M. Bakir, A. M. Lapides, C. J. Dares, T. J. Meyer, *Proc. Natl. Acad. Sci. U.S.A.* **2015**, *112*, 15809-15814.

[19] M. S. Xie, B. Y. Xia, Y. W. Li, Y. Yan, Y. H. Yang, Q. Sun, S. H. Chan, A. Fisher, X. Wang, *Energy Environ. Sci.* **2016**, *9*, 1687-1695.

[20] H. Mistry, A. S. Varela, C. S. Bonifacio, I. Zegkinoglou, I. Sinev, Y. W. Choi, K. Kisslinger, E. A. Stach, J. C. Yang, P. Strasser, B. R. Cuenya, *Nat. Commun.* **2016**, *7*, 12123.

[21] M. Li, J. Wang, P. Li, K. Chang, C. Li, T. Wang, B. Jiang, H. Zhang, H. Liu, Y. Yamauchi, N. Umezawa, J. Ye, *J. Mater. Chem. A* **2016**, *4*, 4776-4782.

[22] T. Takashima, T. Suzuki, H. Irie, *Electrochim. Acta* **2017**, *229*, 415-421.

[23] S. Zhang, P. Kang, M. Bakir, A. M. Lapides, C. J. Dares, T. J. Meyer, *Proc. Natl. Acad. Sci. U. S. A.* **2015**, *112*, 15809-15814.

[24] S. Ma, M. Sadakiyo, M. Heima, R. Luo, R. T. Haasch, J. I. Gold, M. Yamauchi, P. J. A. Kenis, *J. Am. Chem. Soc.* **2017**, *139*, 47-50.

[25] W. Liu, A.-K. Herrmann, D. Geiger, L. Borchardt, F. Simon, S. Kaskel, N. Gaponik, A. Eychmller, *Angew. Chem. Int. Ed.* **2012**, *51*, 5743-5747; *Angew. Chem*. **2012**, *124*, 5841-5846.

[26] H. D. Gesser, P. C. Goswami, *Chem. Rev.* **1989**, *89*, 765-788.

[27] H.-P. Yang, S. Qin, Y.-N. Yue, L. Liu, H. Wang, J.-X. Lu, *Catal. Sci. Technol.* **2016**, *6*, 6490-6494.

[28] X. Sun, Q. Zhu, X. Kang, H. Liu, Q. Qian, Z. Zhang, B. Han, *Angew. Chem. Int. Ed.* **2016**, *55*, 6771–6775; *Angew. Chem.* **2016**, *128*, 6883–6887.

[29] H.-P. Yang, S. Qin, H. Wang, J.-X. Lu, *Green Chem.* **2015**, *17*, 5144-5148.

[30] P. K. Giesbrecht, D. E. Herbert, *ACS Energy Lett.* **2017**, *2*, 549-555.

[31] M. Gattrell, N. Gupta, A. Co, *J. Electroanal. Chem.* **2006**, *594*, 1-19.

[32] Y.-X. Duan, F.-Lu. Meng, K.-H. Liu, S.-S. Yi, S. -J. Li, J. -M. Yan, Q. Jiang, *Adv. Mater.* **2018**, *30*, 1706194.

[33] W. Zhang, Q. Qin, L. Dai, R. Qin, X. Zhao, X. Chen, D. Ou, J. Chen, T. T Chuong, B. Wu, N. Zheng, *Angew. Chem. Int. Ed.* **2018**, *57*, 9475–9479; *Angew. Chem.* **2018**, *130*, 9619–9623.

[34] C. S. Le Duff, M. J. Lawrence, P. Rodriguez, *Angew. Chem. Int. Ed.* **2017**, *56*, 12919-12924.; *Angew. Chem.* **2017**, *129,* 13099-13104.

[35] M. Favaro, H. Xiao, T. Cheng, W. A. Goddard, J. Yano, E. J. Crumlin, *Proc. Natl. Acad. Sci. U. S. A.* **2017**, *114*, 6706-6711.

[36] D. Ren, J.Fong, B. Yeo, *Nat. Commun.* **2018**, *9*, 925.

[37] M. Le, M. Ren, Z. Zhang, P. T. Sprunger, R. L. Kurtz, J. C. Flake, *J. Electrochem. Soc.* **2011**, *158*, E45-E49.

[38] Salehi-Khojin, A.; Jhong, H.-R. M.; Rosen, B. A.; Zhu, W.; Ma, S.; Kenis, P. J. A.; Masel, R. I. *J. Phys. Chem. C* **2013**, *117*, 1627.

10.1002/anie.201808964

WILEY-VCH

Entry for the Table of Contents (Please choose one layout)

COMMUNICATION

Pd-Cu bimetallic aerogel was outstanding electrocatalyst for conversion of CO_2 in CH_3OH in an aqueous solution of ionic liquid. The current density could reach 31.8 mA cm^{-2} with a Faradaic efficiency of 80.0% over $Pd_{83}Cu_{17}$ aerogel electrode at a low overpotential of 0.24 V.

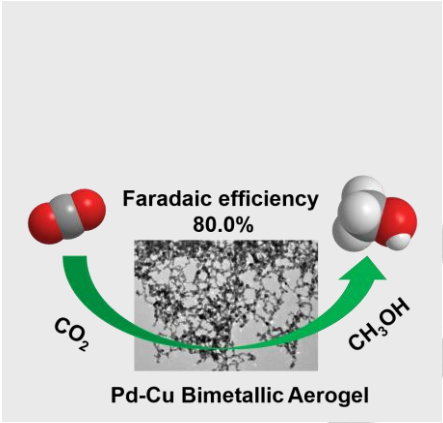

Lu Lu,[a,b] Xiaofu Sun,[a,b] Jun Ma,[a] Dexin Yang,[a,b] Haihong Wu,[c] Binxing Zhang,[a,b] Jianling Zhang,[a,b] Buxing Han[a,b]**

Page No. – Page No.

Highly Efficient Electroreduction of CO_2 to Methanol on Palladium-Copper Bimetallic Aerogels